KINEMATICS OF ENGULFMENT IN A TURBULENT WAKE

Gregory A. Kopp
Boundary Layer Wind Tunnel Laboratory, Faculty of Engineering Science
The University of Western Ontario, London, Ontario, N6A 5B9, Canada

Francesc Giralt, Josep A. Ferré
Departament d'Enginyeria Quimica, ETSEQ, Universitat Rovira i Virgili
Carretera de Salou, s/n, 43006 Tarragona, Catalunya, Spain

James F. Keffer
Department of Mechanical and Industrial Engineering, University of Toronto
5 King's College Road, Toronto, Ontario, M5S 1A4, Canada

ABSTRACT

Hot-wire measurements were made simultaneously in two homogeneous, "horizontal" planes in the far wake region of a cylinder. A technique to identify the spatial characteristics of the large scale bulges at the interface between the internal turbulent motions and the external irrotational flow was developed. Together with the hot-wire data, this technique allowed us to relate unambiguously the outer bulges to the inner coherent structures. Other kinematic features of the engulfment process such as the relative positioning of critical points and the primary locations of inflow to the wake were described.

INTRODUCTION

Understanding the kinematics and dynamics of entrainment is important in many practical engineering situations involving mixing, combustion or the dispersion of contaminants. In these applications, flows tend to be complex and many engineering turbulence models used to predict them break down. The fundamental study of three-dimensional turbulence structures and their related transfer processes in the far region of a plane turbulent wake is relevant to these situations because entrainment and the transfer of momentum, heat and mass that occur in free flows depend strongly on the structure of the internal vortical motions and how these motions interact with the external "irrotational" field.

Entrainment is the process whereby the exterior irrotational fluid is ingested by the interior rotational, turbulent flow. On the one hand, this is accomplished at the turbulent-nonturbulent interface by the diffusion of vorticity at the smallest scales. This is what we mean by mixing. On the other hand, engulfment is also one of the physical processes involved in entrainment, although the details of it are not entirely understood. Engulfment involves the extension of the interface, first described by Corrsin and Kistler (1955), by large scale turbulent motions causing an increase in the overall entrainment rate.

Large scale, coherent structures, have long been associated with the engulfment process (Townsend, 1966). Many of the details pertaining to the coherent structures have since been investigated. Mumford (1983) and Ferré and Giralt (1989) identified the three-dimensional velocity and temperature patterns of the coherent structures in the far wake region. The velocity patterns observed in "horizontal" homogeneous planes were like Grant's (1958) double rollers. Bisset et al. (1990) conditionally-averaged the far wake velocity field in a "vertical" shear plane. The streamlines of their structures led them to construct a kinematic model using Rankine vortices which had double roller type motions in the (horizontal) homogeneous planes.

Recently, Vernet et al. (1999) identified the complete three-dimensional topology of these far wake structures. They found the structure of the *velocity fluctuations* to be shear-aligned, ring-like vortices. Here, the double roller structure represents a horizontal slice through the vortex. However, the true three-dimensional structure of the *flow* (obtained by taking into account the mean shear) is a vortex

in the shape of a tube. It is thought that these vortex tubes are the large scale turbulent bulges.

Falco (1977) inferred an upstream saddle point between the turbulent bulge/large scale structure and the freestream in a boundary layer. Similarly, but in a cylinder wake, Vernet et al. (1999) identified a saddle point upstream of the coherent structure, near the location of maximum shear, within the fully turbulent zone.

In this paper we present various details pertaining to the engulfment process related to the far wake coherent structures and the turbulent bulges. After reviewing the prototypical coherent structure found by Vernet et al. (1999), a technique for identifying turbulent bulges is presented. Data obtained simultaneously in two planes is used so that the positioning of the (outer) bulges, along with the quiescent, irrotational zones relative to the (inner) coherent structures can be examined.

EXPERIMENTAL DETAILS

Measurements were made in a plane turbulent cylinder wake in the open return wind tunnel at the Universitat Rovira i Virgili in Tarragona. This facility has a test section 60x60 cm square and 300 cm long. The diameter of the cylinder, D, was 11.6 mm (aspect ratio of 40 and tunnel blockage of 2.0%) while the freestream velocity, U_o, was 9 m/s, so that the Reynolds number was 6700. The freestream turbulence intensity was less than 0.2%. The cylinder was mounted through holes in the tunnel walls.

Figure 1 shows a sketch of the setup. A fixed rake of 4 X-wires was placed 170 diameters downstream of the cylinder at $y=l_o$, where l_o is the mean velocity half-width, to measure the u+w velocity components. The probe spacing was $\Delta z = 0.33\ l_o$. A second fixed rake of 8 normal wires was placed immediately above the X-wire rake at $y=l_h$, where l_h is the half-intermittency point, to measure the streamwise velocity components immediately above the X-wire rake. The probe spacing for the normal wire rake was $\Delta z = 0.14\ l_o$. Note that both rakes have the same spanwise extent. The voltage signals from each anemometer were low-pass filtered at 2 kHz and sampled at 5000 samples/s for 40 s ($\Delta\tau$=0.2 ms). The data were stored on optical disks.

There are several points to note. First, the spatial coordinates are normalized according to $z^* = z/l_o$, $y^* = y/l_o$ and $x^*=-U_o t/l_o$. The conversion of the time coordinate to the streamwise coordinate requires the use of Taylor's hypothesis of frozen turbulence. We have used freestream velocity for this conversion. Second, flow is from left to right in all plots. Third, the mean velocity half width length scale is l_o = 42 mm, while the half intermittency point is $y = l_h$ = 67 mm = 1.6 l_o. The integral scale is 3.2 ms (= 0.7 l_o assuming Taylor's hypothesis). Fourth, the velocity fluctuations are normalized by the local rms. value, u* = u/u'. Finally, triangular brackets, <>, indicate an ensemble-average.

FEATURES OF THE PROTOTYPICAL COHERENT STRUCTURE

The three-dimensional topology of the prototypical coherent structure was recently "visualized" by Vernet et al. (1999). To do this, the vortex identification technique of Jeong and Hussain (1995) was used, with the results shown in Fig. 2. This figure shows both the ensemble-averaged velocity fluctuation vectors in two planes and the outline of the coherent vortex in gray, "visualized" with Jeong and Hussain's (1995) technique, in the same planes. For the latter, it was assumed that all of the mean shear was due to the coherent motions.

The well known double roller structure (e.g., Grant, 1958) is simply a horizontal slice near the wake half-width (i.e., $y \approx l_o$) as can be inferred by examining Fig. 2b. Grant's (1958) mixing jet structure is in the symmetry plane of the double roller structure (Vernet et al., 1999). Interestingly, the coherent vortex (outlined in gray) does not cover what the entirety of the double roller/mixing jet structure, being somewhat smaller.

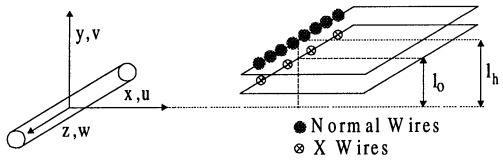

Figure 1. Definition sketch.

FEATURES OF THE LARGE SCALE TURBULENT BULGES

Assumptions of the Bulge Identification Technique

In order to identify the large scale bulges from discrete experimental data several assumptions need to be made. First, we are neglecting small scale bulges. At present, our work is not concerned with small scale measures of the interface such as fractal dimensions. Our objective, rather, is to identify large scale bulges and coherent structures simultaneously in order to gain information about the engulfment mechanism and entrainment. Nevertheless, all intermittency work is concerned with the small scales at some level because the interface is thin, Thus, our intermittency function must be obtained over a small enough time scale so that the interface is carefully resolved.

Possibly the most critical assumption is that when two adjacent data points indicate rotational flow, the spatial locations between the two are assumed to be rotational. This is implicitly assumed in the calculation of the intermittency function from the time series of a single probe which utilizes a hold time as a form of smoothing in order to obtain better estimates of the intermittency function (e.g., Tabatabai et al., 1989). However, the assumption becomes explicit when examining the spatial distribution of the intermittency function obtained from multiple probes separated in space.

Difficulty arises if the bulges are assumed to contain any sort of porosity, or locations where the intermittency function is zero, indicating the presence of irrotational fluid, because a threshold will then be required to determine whether or not any given "event" is a bulge. However, if engulfment occurs, it seems probable that there be irrotational zones contained within what is considered to be a bulge.

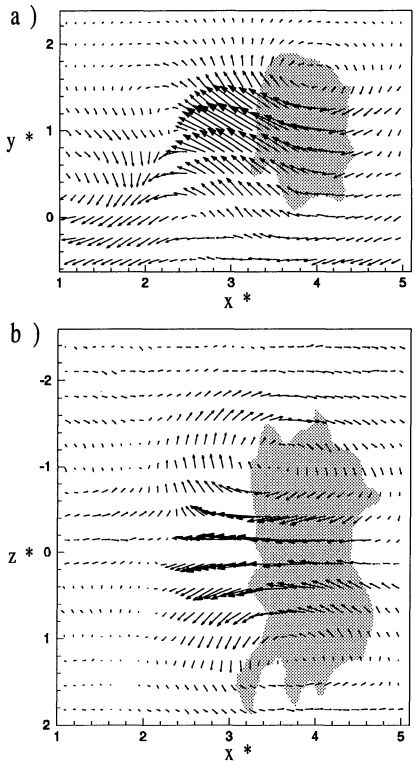

Figure 2. View of the 5% isocontours of λ_2 with the coherent velocities in the (a) x*-y* plane at z* = -0.14, and (b) x*-z* plane at y* = 1.0. Data from Vernet et al. (1999).

In order to identify real bulges the time series of the turbulence indicator function for the eight sensors at $y = l_h$ were examined. Figure 3 depicts a segment of these time series with the white zones indicating turbulent flow (I = 1) and the black zones indicating irrotational flow (I = 0). In can be observed that there are a few irrotational "patches" surrounded by turbulent flow. In addition, at the downstream end of the figure, the interface is generally observed to be continuous in the plane (applying the assumptions described above) but that it undulates significantly. Because of the limited spatial resolution obtained with the rake of hot-wires, one can not possibly hope to identify the actual edge of the bulges. Rather, the technique is based on identifying the "bulk features" of the bulges.

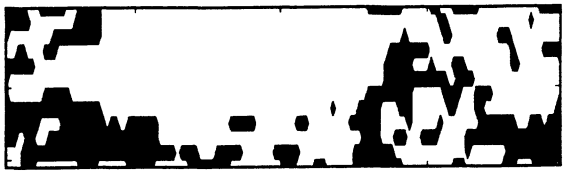

Figure 3. Time series of the turbulence indicator function obtained from the eight probes located at $y = l_h$.

Like the intermittency function itself, every technique which is developed to identify bulges from discrete intermittency function data is dependent on the numerical value of the threshold selected. However, one would expect that the actual kinematics of the bulges would be a factor in its identification. Consider, for example, a hypothetical intermittency function for a single probe. A bulge of considerable streamwise extent is illustrated as the uppermost signal in Fig. 3. Several possibilities can exist for the signals from closely spaced adjacent probes.

First, an adjacent probe could yield a similarly long period of rotational flow. In this case, the only assumption to be made is whether the intervening space is also rotational. A threshold close to unity could be applied here.

Second, it could yield a series of shorter bursts. Without continuous spatial information between the probes one is left to infer the significance of this situation. The most reasonable scenario is that these events are physically connected and the bursts in this second probe represent solid regions of a continuous large scale bulge, while the quiescent zones represent porosity, or holes, within the bulge. Of course, as the quiescent zones become longer, and the bursts shorter, in the adjacent probe, the likelihood that they are part of the same bulge diminishes.

When engulfment occurs, one would expect there to be porosity, or patches, within the bulges. In this case, a

threshold near unity would not detect the presence of many bulges because there would not be many bulges that are completely solid in this situation. Thus, one expects a threshold somewhat less than unity. However, it seems likely that the threshold should also be greater such that greater than 50% of the nominal bulge area is rotational.

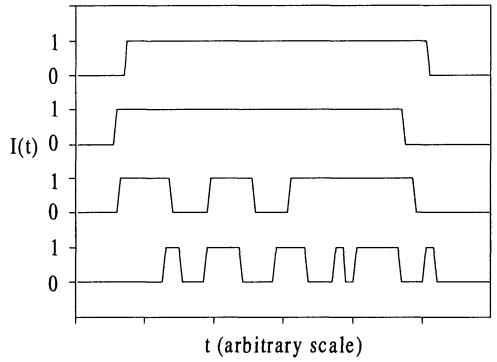

Figure 4. Possible scenarios for determining when the intermittency function from adjacent probes are due to a single bulge.

Identification of Large Scale Bulges

In order to identify large-scale turbulent bulges we developed a technique based on spatially averaged intermittency functions. In particular, two spatial averages are used; one of a larger scale to identify when there is a large scale bulge present,

$$I_{ls}(\vec{x},t) = \frac{1}{n_{ls}n_z} \sum_{i=1}^{n_{ls}} \sum_{k=1}^{n_z} (I_{i,k}(\vec{x},t)) \qquad (1)$$

and one of a smaller scale one to determine the approximate location of the edge of the bulge (with I_{ss} and n_{ss} replacing I_{ls} and n_{ls} in equation 1). Here, I_{ls} is the large scale spatially-averaged intermittency factor, n_{ls} is the number of data points used in time (approximating the streamwise direction) and n_z is the number of probes used in the spanwise direction. I_{ss} and n_{ss} are defined as above but are of a smaller scale. The intermittency function is determined in the present work using the technique and detector function of Tabatabai et al. (1989),

$$D(t_j) = \left\{(U_j - U_o)\left(\frac{\Delta U_j}{\Delta t}\right)\right\}^2 \qquad (2)$$

It is assumed that there is a large scale bulge present when I_{ls} is near unity and that a quiescent (irrotational) region is present when I_{ls} approaches zero. We thus use I_{ls} to determine when a bulge is present with a threshold set to an appropriate value. In this case, the threshold used in the determination of the bulges was that $I_{ls} > 0.70$ at some point within the bulge. In order to identify the front and back edges of the bulges the smaller scale spatially averaged intermittency is used. In particular, once $I_{ss} < 0.30$, it is assumed that the edge has been identified.

We found that the actual value of n_{ls} (= 19 ~ 1.3 integral scales) was not critical as long as it was chosen to represent the smallest of the large scale bulges but was not so large that I_{ls} approached the global average at that location. We used $n_{ss} = 3$ (~ 0.2 integral scales).

Using this technique turbulent bulges and quiescent regions were identified with the normal wire data at $y = l_h = 1.6\ l_o$. In this way, 42% of the flow was classified as being bulges of a size greater than 0.7 integral scales and 35% of the flow was classified as quiescent, with 30% of the flow being quiescent regions of a size greater than 0.7 integral scales. The remainder of the flow was unclassified. Table 1 gives additional statistics relating to these regions. Interestingly, the amount of flow classified as "bulges" is similar to the fraction of the flow occupied by double roller (Giralt and Ferré, 1993).

Positioning of Large Scale Bulges Relative to the Coherent Structures

Figure 5 shows a sample of the results obtained with the present experimental data. All bulges were grouped according to size. Figures 5a-c show ensemble-averages obtained for bulges of a streamwise extent of l_o, 3 l_o and 4 l_o, respectively. In these figures the contour levels are of <u*> at $y = l_h$ for the bulges identified. The vectors are of <u*,w*> at $y = l_o$. It must be emphasized that these are the average motions occurring simultaneously in time, but physically separated in the lateral direction by 0.6 l_o (1.1 integral scales). Note that the lateral location $y = l_o$ is approximately at the edge of the fully turbulent zone.

TABLE 1. STATISTICS PERTAINING TO THE TURBULENT BULGES AND QUIESCENT REGIONS

	bulges	**quiescent regions**
fraction of flow	41.9%	35.1%
fraction of intermittency	74.2%	3.5%
fraction of $\overline{u^2}$	87.2%	3.2%
fraction of $(\partial u/\partial t)^2$	83.9%	3.8%

Several observations can be made from Figs. 5a-c. First, within the outer bulges, at $y = l_h$, the largest negative streamwise fluctuations occur nearer the backside (or upstream edge) of the bulges while the largest positive streamwise fluctuations occur nearer to the fronts (or

downstream edge). The larger the bulge, the more energetic it is.

Second, when there is a bulge present at the edge of the wake, the interior motions consist of negative streamwise velocity fluctuations. The larger the bulge, the larger the magnitude of the interior velocity fluctuations.

These observations indicate that the motions in the fully turbulent core of the wake associated with outer bulges are the same motions that occur in the mixing jet region of the double roller structure. In other words, this is the region with negative <u*> in Fig. 2. These motions are well correlated with outward lateral velocity fluctuations (Fig. 2; see also Vernet et al., 1999). This is not suprising as it has long been expected that the double roller portion of the ring-like vortex forms the base of the turbulent bulges (e.g., Ferré and Giralt, 1989; Giralt and Ferré, 1993).

In addition, it seems likely that the larger bulges have emerged further from the core of the wake and, therefore, are relatively more energetic with correspondingly higher levels of fine scale turbulence and dissipation. In this case, engulfment occurs further from the wake core. Similarly, the smaller bulges may be ones which have not emerged quite as far. These are less energetic and are the tops of bulges which are either smaller or closer to the wake centreline. In this case, the engulfment occurs closer to the wake centreline.

Positioning of Large Scale Quiescent Regions Relative to the Coherent Structures

Figure 6 shows a sample of the results obtained from the identification of the quiescent (irrotational) regions at $y = l_h$. Again, these zones were grouped according to their size and ensemble-averaged. Figure 6 shows the results for zones of a streamwise extent of 2 l_o. This figure is characteristic for all sizes.

The most important observation that can be made is that when there is a zone of irrotational flow at $y = l_h$, there are positive <u*> within the fully turbulent core at $y = l_o$. Comparing Fig. 2 and Fig. 6 it is observed that the quiescent zones occur simultaneously with the outer spanwise edges of the double roller structure. A second observation is that at $y = l_h$ there is little variation of <u*>, consistent with this being (external) irrotational flow.

Positioning of Critical Points

Figure 7 shows a simplified sketch summarizing the present results, together with those in Vernet et al. (1999) and Ferre-Gine et al. (1997). In reality, there is randomness in each aspect of the entrainment process, so that this figure depicts only the average process. The heart of the figure is the double roller eddy, which we have already shown to be a horizontal slice of a the large scale vortex tube. In its centre is Grant's (1958) mixing jet with a net outflow of fine-scale turbulence. This outflow is originating from the core of the wake below the double roller. Inflow, or engulfment, occurs primarily at the outer edges of the double roller. Streamwise velocity fluctuations are correlated with lateral velocity fluctuations for both inflow and outflow. It is important to note that the scale of the structure is large, and the motions relatively slow, so that the structure must be significantly evolved before this newly engulfed fluid is ejected.

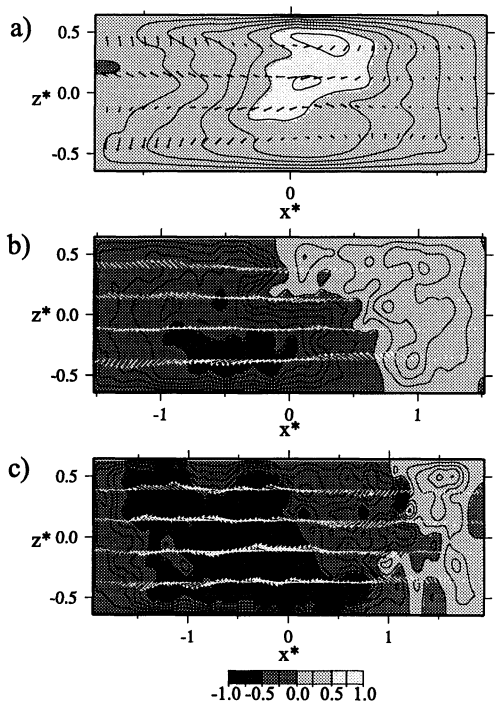

Figure 5. Velocity fluctuations associated with the turbulent bulges in two planes. Contours are <u*> at $y = l_h$, while vectors are <u*> + <w*> at $y = l_o$. The maximum and minimum of <u*> at $y = l_h$ are, respectively, (a) 0.62 and -0.01, (b) 0.34 and -0.67, and (c) 0.41 and -1.13.

Upstream of the double roller is a saddle point (see Fig. 2; also Ferre-Gine et al., 1997) and upstream of the saddle point is more inflow. This inflow is part of another vortex, either a double roller or single roller. Ferre-Gine et al. (1997) found that there is either a double roller, or single rollers of either clockwise or counter-clockwise rotation associated with this inflow. However, the ensemble-averages of these motions lead us to believe that these single rollers are part of double rollers which fall outside of the width of the data (see also Ferré and Giralt, 1989 for a discussion of single rollers and double rollers).

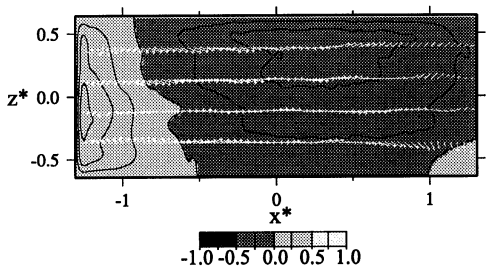

Figure 6. Velocity fluctuations associated with quiescent zones in two planes. Contours are <u*> at y = l_h while vectors of <u*,w*> at y = l_o. The maximum and minimum of <u*> are 0.35 and -0.23, respectively.

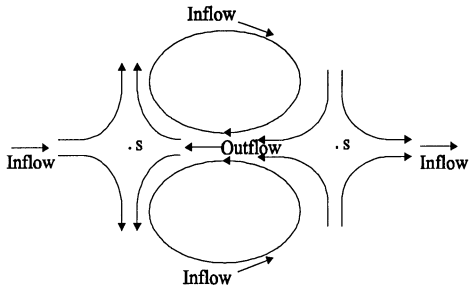

Figure 7. Sketch of the engulfment process in a horizontal plane.

There is also evidence for a downstream saddle point, although this evidence is weaker, possibly because the downstream edge is not as sharp as the upstream edge (Ferré and Giralt, 1989; and others). There is also no apparent shear-alignment at the downstream edge. Downstream of this saddle point there is also inflow into another vortex structure. The same orientation issues described in the paragraph above come into play here.

Finally, as pointed out by Ferre-Gine et al. (1997), the double roller/ring-like vortex configuration is a real instantaneous structure and is not just an artefact of the averaging procedure. One reason that this configuration is stable may be because the external irrotational flow moves around it on either side of the ring-like vortex as it emerges (as a bulge).

CONCLUSIONS

Turbulent bulges and quiescent, irrotational zones have been identified in the far wake region of a circular cylinder and related to the prototypical coherent structure in this region. Kinematic details pertaining to the process of engulfment in and around the coherent structure and it's critical points have been found. These include the locations where engulfment actually occurs. Inflow occurs all around the bulges, and is particularly associated with the upstream and downstream saddle points on either side of the structure. Inflow at the spanwise ends of the coherent structure may stabilize the double roller pattern and explain its existence.

ACKNOWLEDGMENTS

Thanks are accorded to Dr. A. Vernet for his assistance with the plots. This work was financially supported by DGICYT project PB96-1011, NATO Collaborative Research Grant 960142 and the National Sciences and Engineering Research Council of Canada.

REFERENCES

Bisset, D.K., Antonia, R.A. and Browne, L.W.B., 1990, "Spatial organization of large structures in the turbulent far wake of a cylinder," *Journal of Fluid Mechanics*, vol. 218, pp. 439-461.

Corrsin, S. and Kistler, A.L., 1955, "Free-stream boundaries of turbulent flows," NACA report 1244.

Falco, R.E., 1977, "Coherent motions in the outer region of boundary layers," *Physics Fluids*, vol. 20, pp. S124-S132.

Ferré, J.A. and Giralt F., 1989, "Some topological features of the entrainment process in a heated turbulent wake," *Journal of Fluid Mechanics,* vol. 198, pp. 65-77.

Ferre-Gine, J., Rallo, R., Arenas, A. and Giralt, F., 1997, "Extraction of structures from turbulent signals," *Artificial Intelligence in Engineering*, vol. 11, pp. 413-419.

Giralt, F. and Ferré, J.A., 1993, "Structure and flow patterns in turbulent wakes," *Physics of Fluids (A),* vol. 5, pp. 1783-1789.

Grant, H.L., 1958, "The large eddies of turbulent motion," *Journal of Fluid Mechanics,* vol. 4, pp. 149-190.

Jeong, J. and Hussain, F., 1995, "On the identification of a vortex," *Journal of Fluid Mechanics,* vol. 285, pp. 69-94.

Mumford, J.C., 1983, "The structure of the large eddies in fully developed turbulent shear flows. Part 2. The plane wake," *Journal of Fluid Mechanics,* vol. 137, pp. 447-456.

Tabatabai, M., Kawall, J.G. and Keffer, J.F., 1989, "Choice of the threshold in a velocity-based conditional sampling procedure," *Phys. Fluids (A),* vol. 1, pp. 307-311.

Townsend, A.A., 1966, "The mechanism of entrainment in free turbulent flows,", *Journal of Fluid Mechanics*, vol. 26, pp. 689-715.

Vernet, A., Kopp, G.A., Ferré, J.A., and Giralt, F., 1999, "Three-dimensional structure and momentum transfer in a turbulent cylinder wake," submitted to *Journal of Fluid Mechanics*.